

## Measurement of scattering cross sections of $^{nat}\text{Pb}$ at an incident neutron energy of 2.94 MeV

E. Pönitz<sup>a</sup>, R. Nolte, and D. Schmidt

Physikalisch-Technische Bundesanstalt, 38116 Braunschweig, Germany

**Abstract.** At the PTB TOF spectrometer, cross sections were measured for the elastic and inelastic scattering of neutrons on  $^{nat}\text{Pb}$  at an incident neutron energy of  $E_n = 2.94\text{ MeV}$ . The  $^{15}\text{N}(p,n)^{15}\text{O}$  reaction was used for the production of monoenergetic neutrons. Measurements were carried out at 10 angles from  $25^\circ$  to  $130^\circ$ . Angle-integrated cross sections were obtained by fitting a Legendre polynomial expansion to the experimental data. Cross sections could be determined for the elastic scattering on  $^{nat}\text{Pb}$  as well as for inelastic scattering with excitation of the 1<sup>st</sup> level of  $^{206}\text{Pb}$  and the 1<sup>st</sup> and 2<sup>nd</sup> level of  $^{207}\text{Pb}$ . The cross sections were normalized to the ENDF/B-V hydrogen scattering cross section. The preliminary results are compared with existing experimental and evaluated data, i.e. cross section data of the ENDF/B-VI.8 and JENDL 3.3 evaluations. Additional measurements in the energy range from 2 MeV to 4 MeV are in progress.

### 1 Introduction

Reliable cross section data are required for lithium-lead tritium-breeding blankets for fusion reactors and for Accelerator-Driven Systems (ADS). In particular the neutron transport in a lead spallation target is strongly dependent on the inelastic neutron scattering cross sections between 1 MeV and 4 MeV [1, 2].

So far, the PTB time-of-flight (TOF) spectrometer has already been used to measure differential and double-differential cross sections for lead in the energy range from 8 MeV to 14 MeV [3]. For these measurements, a  $\text{D}_2$  gas target was used for the production of neutrons by the  $\text{D}(d,n)$  reaction. Recently, the energy range was extended to lower energies by using the  $^{15}\text{N}(p,n)^{15}\text{O}$  reaction. With this reaction, monoenergetic neutrons with energies up to 5.7 MeV can be produced. NE213 liquid scintillation detectors were used for neutron detection. The data analysis is based on a realistic simulation of the measured TOF spectra. This procedure as well as the detailed description of the detector properties (time response, pulse height response) allow a very reliable determination of the cross sections.

In a first experiment, differential elastic and inelastic scattering cross sections were measured at an energy of  $E_n = 2.94\text{ MeV}$  using a  $^{nat}\text{Pb}$  sample. Cross sections were determined for the elastic scattering on  $^{nat}\text{Pb}$  as well as for the inelastic scattering with excitation of the 1<sup>st</sup> excited level of  $^{206}\text{Pb}$  and the 1<sup>st</sup> and 2<sup>nd</sup> level of  $^{207}\text{Pb}$ . Differential cross sections were determined at 10 angles from  $25^\circ$  to  $130^\circ$ . Angle-integrated cross sections were obtained by fitting a Legendre polynomial expansion to the experimental data points. The experimental data were normalized to the ENDF/B-V hydrogen scattering cross section.

### 2 The PTB TOF spectrometer

An overview of the PTB TOF spectrometer is shown in figure 1. The cyclotron (denoted by CY) can be rotated from  $-20^\circ$  to  $+110^\circ$  with respect to detector D1, resulting in scattering angles between  $0^\circ$  and  $160^\circ$ . Pulsed beams with a time width of 0.8 ns to 2.0 ns can be produced. The gas target T has a length of 3 cm. Its entrance window consists of a  $5\text{ }\mu\text{m}$  Mo-foil. The scattering sample S is located at the pivot point. The flight path of the scattered neutrons is 12 m. The distance between the centre of the gas target and the pivot point is 17.5 cm. The detectors D1 ( $\text{Ø } 4'' \times 1''$ ), D2–D5 ( $\text{Ø } 10'' \times 2''$ ) and the neutron fluence monitor detector M are NE213 liquid scintillation detectors which are sensitive to  $\gamma$  rays and fast neutrons. A detailed description of the PTB TOF spectrometer can be found in ref. [4].

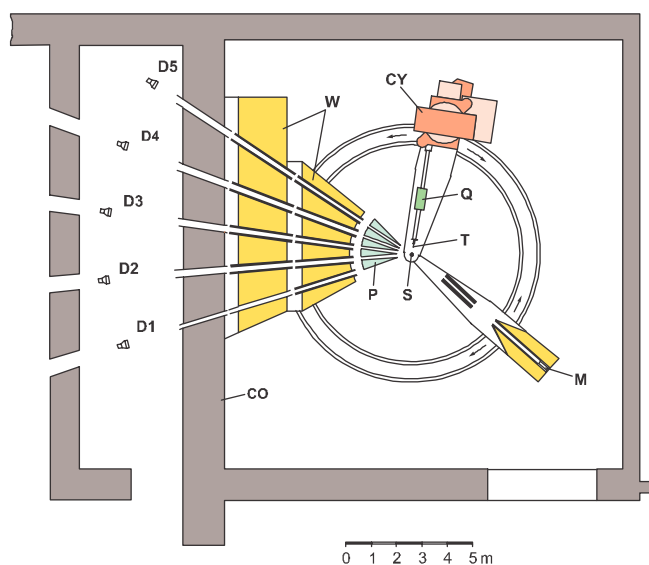


Fig. 1. Schematic view of the PTB TOF spectrometer (see text).

<sup>a</sup> Presenting author, e-mail: Erik.Poenitz@ptb.de

### 3 The $^{15}\text{N}(p,n)^{15}\text{O}$ reaction as a source for monoenergetic neutrons

Neutron scattering cross sections have been determined with high precision at PTB for more than twenty years. So far, primarily the  $\text{D}(d,n)$  reaction has been used for the production of neutrons. Due to the  $Q$  value of  $+3.27$  MeV and the deuteron energies available at the cyclotron, neutrons in the energy range from 6 MeV to 16 MeV can be produced. For the measurement of neutron scattering cross sections below 6 MeV, however, the implementation of a new neutron source was necessary.

With the  $^{15}\text{N}(p,n)$  reaction, monoenergetic neutrons with energies up to 5.7 MeV can be produced because the energy  $E_1$  of the 1<sup>st</sup> excited state of  $^{15}\text{O}$  is 5.18 MeV. A gas target allows background subtraction by gas-in/gas-out difference measurements as well as the easy variation of the target thickness by changing the gas pressure.  $^{15}\text{N}$  is a stable isotope and the produced  $^{15}\text{O}$  activity does not pose a radiological problem due to its short half life  $T_{1/2} = 122$  s. In contrast to this, the use of the  $\text{T}(p,n)$  reaction which is commonly used for the production of neutrons in the few MeV region is not possible at the PTB TOF spectrometer because of the radioactive hazard.

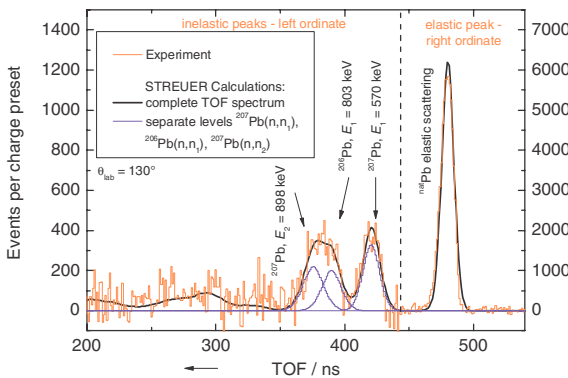


**Fig. 2.** Simulated and measured TOF spectra of neutrons scattered from a  $^{\text{nat}}\text{Pb}$  sample for a scattering angle  $\theta_{\text{lab}} = 130^\circ$ . Note the different ordinates for the elastic peak (right axis) and the inelastic peaks (left axis).

A disadvantage of this reaction is the large energy loss of protons in  $^{15}\text{N}_2$  gas compared to that of deuterons in  $\text{D}_2$  gas which causes a reduced neutron yield. In addition, due to the strong resonance structure of the reaction cross section, scattering experiments are only meaningful at selected energies.

For a  $^{\text{nat}}\text{Pb}$  sample, cross section measurements are limited to an incident neutron energy range of 2 MeV to 4 MeV. The lower limit is given by the decrease of the detection efficiency around 1.5 MeV for a detection threshold of about 0.9 MeV which is caused by the properties of the large scintillation detectors. The upper limit is given by the inelastic cross sections which are decreasing with increasing neutron energy. Because of the lowered neutron yield reliable neutron cross section measurements using the  $^{15}\text{N}(p,n)$  reaction are limited to the differential cross sections  $d\sigma/d\Omega$  greater than 10 mb/sr.

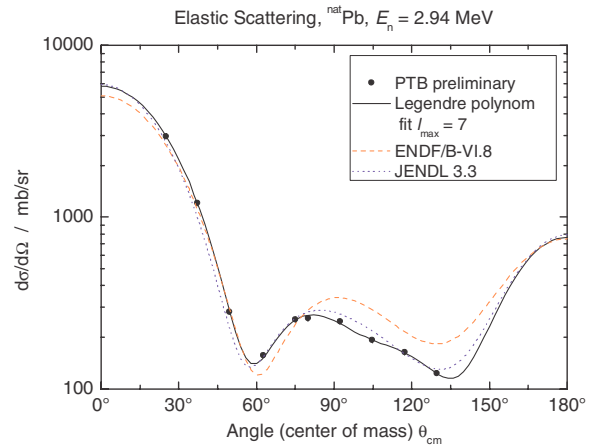


**Fig. 3.** Angular distribution of the elastic scattering on  $^{\text{nat}}\text{Pb}$ . The data from the ENDF/B-VI.8 and JENDL 3.3 evaluations are included for comparison [6]. The uncertainties are smaller than the size of the data points.

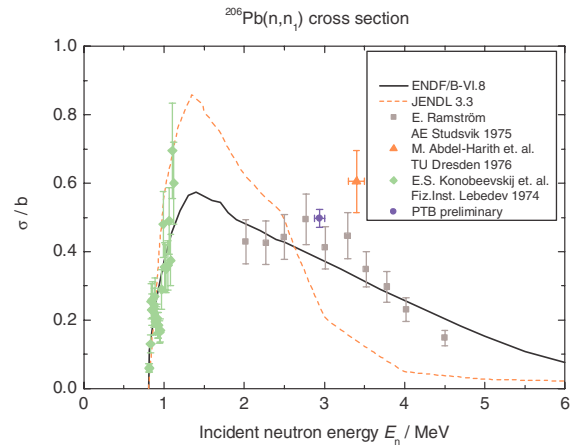


**Fig. 4.** Angle-integrated cross section for inelastic scattering with excitation of the 1<sup>st</sup> level of  $^{206}\text{Pb}$  ( $E_1 = 803$  keV). Experimental data and data from the ENDF and JENDL evaluation are included for comparison [6–9].

The measurements reported in this work are the first measurements of scattering cross sections using the  $^{15}\text{N}(p,n)$  reaction as a neutron source. Therefore, an incident neutron energy in the middle of the energy range of 2 MeV to 4 MeV was chosen.

### 4 Measurements and data analysis

The  $^{15}\text{N}(p,n)$  source was used to carry out neutron scattering measurements at a neutron energy of  $E_n = (2.94 \pm 0.06)$  MeV on a  $^{\text{nat}}\text{Pb}$  sample by the time-of-flight method. The energy spread is primarily caused by the target thickness ( $\Delta E_g \approx 0.09$  MeV) and the energy spread of the proton beam ( $\Delta E_{\text{acc}} \approx 0.06$  MeV FWHM). The lead sample is a full cylinder ( $\varnothing = 2.502$  cm, height  $h = 5.002$  cm, mass  $m = 278.260$  g) with a chemical purity of 99.9%. As in ref. [3], a natural isotopic abundance is assumed. The lead cross sections were normalized to the ENDF/B-V hydrogen scattering cross

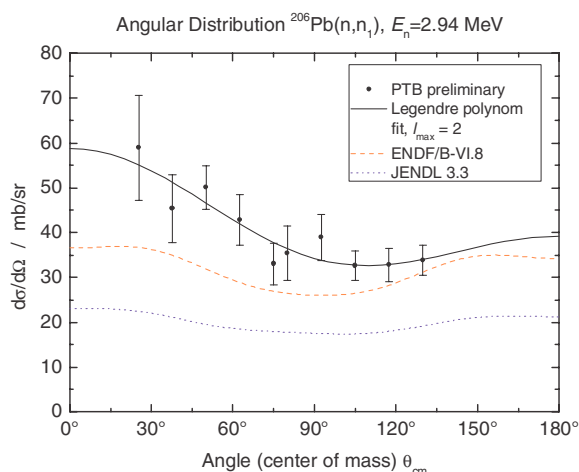


**Fig. 5.** Angular distribution of the inelastic scattering with excitation of the 1<sup>st</sup> level of  $^{206}\text{Pb}$ . The data from the ENDF and JENDL evaluation are included for comparison.

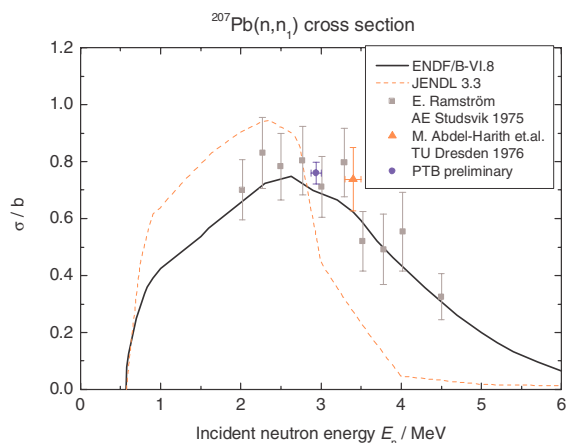


**Fig. 6.** Same as figure 4, but for the 1<sup>st</sup> level of  $^{207}\text{Pb}$  ( $E_1 = 570$  keV).

section. For this measurement, a polyethylene sample ( $\varnothing = 2.456$  cm,  $h = 4.974$  cm,  $m = 22.455$  g, hydrogen mass content = 14.30%) was used.

The data analysis is carried out by iteratively fitting a realistic Monte Carlo simulation of the neutron production, scattering and detection process to the measured time-of-flight spectra. The Monte Carlo code STREUER [5] was used for this simulation. With the simulation, data are corrected for finite geometry, multiple scattering and flux attenuation in the sample and the surrounding air. Figure 2 shows a simulated and a measured TOF spectrum as an example. The measured spectrum is corrected for empty-target background and scattering from air and sample holder.

## 5 Results

Cross sections were determined at 10 angles from 25° to 130° for the elastic scattering on  $^{nat}\text{Pb}$  as well as for the inelastic scattering with excitation of the 1<sup>st</sup> level of  $^{206}\text{Pb}$  (excitation energy  $E_1 = 803$  keV) and the 1<sup>st</sup> and 2<sup>nd</sup> level of  $^{207}\text{Pb}$

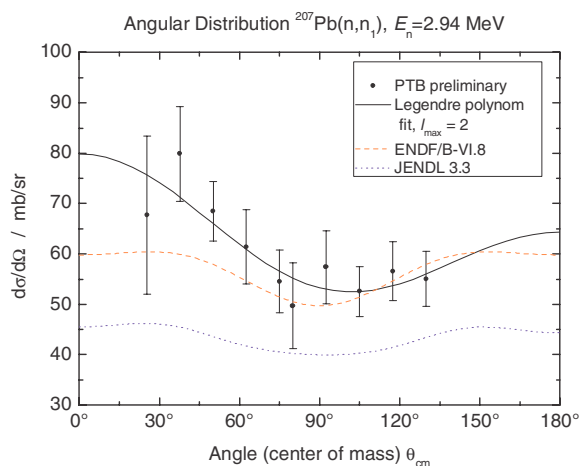


**Fig. 7.** Same as figure 5, but for the 1<sup>st</sup> level of  $^{207}\text{Pb}$ .

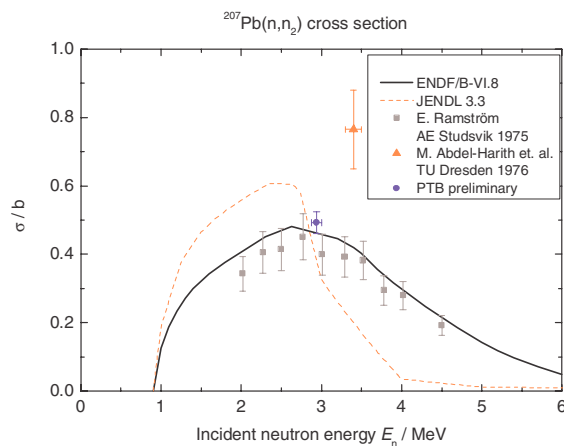


**Fig. 8.** Same as figure 4, but for the 2<sup>nd</sup> level of  $^{207}\text{Pb}$  ( $E_2 = 898$  keV).

( $E_1 = 570$  keV and  $E_2 = 898$  keV, respectively). Angle-integrated cross sections were obtained by fitting a Legendre polynomial expansion to the experimental data using least-squares methods. Figure 3 shows the angular distribution of the elastic scattering on  $^{nat}\text{Pb}$ . Compared with the ENDF/B-VI.8 [6] evaluation, the measured angular distribution is more forward-peaked. The JENDL 3.3 [6] evaluation shows a better agreement. Both ENDF and JENDL integral cross sections show a strong structure of narrow resonances. Averaged over the experimental energy spread, the determined integral cross section  $\sigma_{\text{el}} = (6.70 \pm 0.15)$  b shows a better agreement with the ENDF ( $\sigma_{\text{el}} = 6.72$  b) than with JENDL ( $\sigma_{\text{el}} = 6.45$  b) data.

The results of this measurement for the 1<sup>st</sup> excited level of  $^{206}\text{Pb}$  compared with data from the ENDF and JENDL evaluations as well as with other experimental data [7–9] are shown in figure 4. The data analysis is not yet completed. Preliminary results show that the integrated cross sections are in good agreement with Ramström's measurements [7]. However, smaller uncertainties than in the earlier experimental data could be achieved. For the integrated cross sections, the relative uncertainties are 2% for elastic scattering and about 6% for inelastic scattering. These values include the uncertainties for the energy dependence of the detector efficiencies as well as for the normalization, i.e. the uncertainty of the

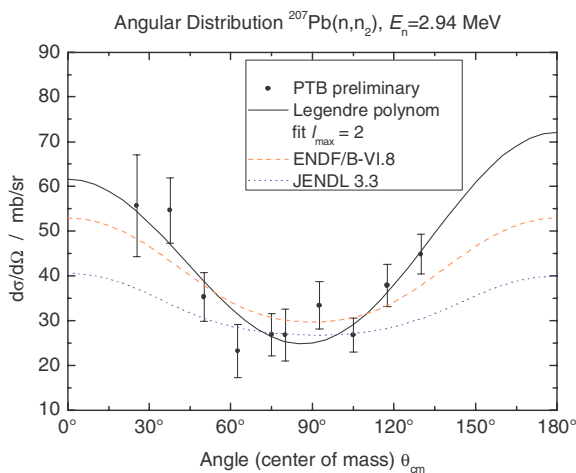


Fig. 9. Same as figure 5, but for the 2<sup>nd</sup> level of <sup>207</sup>Pb.

hydrogen scattering cross section. Figure 5 shows the angular distributions for the 1<sup>st</sup> level of <sup>206</sup>Pb. Figures 6–9 show the results for the 1<sup>st</sup> and 2<sup>nd</sup> level of <sup>207</sup>Pb, respectively.

The angular distributions of both the ENDF and JENDL evaluations are nearly symmetric around 90°. In contrast to this, the measurements for the 1<sup>st</sup> level of <sup>206</sup>Pb and the 1<sup>st</sup> level of <sup>207</sup>Pb are slightly forward-peaked. For all levels, the measured cross sections are in better agreement with the data of ENDF than with the data of JENDL. Additional measurements in the energy range from 2 MeV to 4 MeV are in progress.

## 6 Summary

Scattering cross sections were measured for a <sup>nat</sup>Pb sample at an incident neutron energy of  $E_n = 2.94$  MeV. Angular differential and integrated cross sections were determined for elastic scattering as well as for inelastic scattering at the 1<sup>st</sup> level of <sup>206</sup>Pb and the 1<sup>st</sup> and 2<sup>nd</sup> level of <sup>207</sup>Pb. The

measurements confirm the measurements of inelastic cross section by Ramström but have smaller uncertainties.

Additional measurements in the energy range from 2 MeV to 4 MeV are in progress.

## References

1. M. Embid, R. Fernández, J.M. García-Sanz, E. González, *Systematic Uncertainties on Monte Carlo Simulation of Lead Based ADS Actinide and Fission Product Partitioning and Transmutation*, in *Proceedings of the Fifth International Information Exchange Meeting, Mol, Belgium, 25–27 Nov. 1998*.
2. G. Aliberti, G. Palmiotti, M. Salvatore, C.G. Stenberg, *Impact of Nuclear Data Uncertainties on Transmutation of Actinides in Accelerator-Driven Assemblies*, *Nucl. Sci. Eng.* **146**, 13 (2004).
3. D. Schmidt, W. Mannhart, H. Xia, *Differential Cross Sections of Neutron Scattering on Elemental Lead at Energies between 8 MeV and 14 MeV*, Report PTB-N-27, Braunschweig 1996, ISBN 3-89429-802-2.
4. D. Schmidt, H. Klein, *Precise Time-of-Flight Spectrometry of Fast Neutrons – Principles, Methods and Results*, Report PTB-N-35, Braunschweig 1998, ISBN 3-89701-237-5.
5. D. Schmidt, B.R.L. Siebert, *Fast Neutron Spectrometry and Monte Carlo Simulation – The Codes SINENA and STREUER*, Report PTB-N-40, Braunschweig 2000, ISBN 3-89701-531-5.
6. ENDF/B-VI.8 and JENDL 3.3 data taken from the JANIS-2.1, DVD-ROM distributed by NEA, 2004.
7. E. Ramström, *A Systematic Study of Neutron Inelastic Scattering in the Energy Range 2.0 MeV to 4.5 MeV*, EXFOR 20788, Experimental data taken from the EXFOR database, JANIS-2.1 DVD-ROM distributed by NEA, 2004.
8. M. Abdel-Harith et al., *Elastic and Inelastic Scattering of 3.4 MeV Neutrons by V-51, Co-59 and Pb-206,207*, EXFOR 30464, Experimental data taken from the EXFOR database, JANIS-2.1 DVD-ROM distributed by NEA, 2004.
9. E.S. Konobeevskij et al., *Neutron Inelastic Scattering on Nuclei of Hg-198,200,202, Pb-206 in Energy Range near Threshold*, EXFOR 40215, Experimental data taken from the EXFOR database, JANIS-2.1 DVD-ROM distributed by NEA, 2004.